Desalination and Water Treatment
www.deswater.com
doi: 10.1080/19443994.2014.1003972

57 (2016) 5687–5699
March

Taylor & Francis
Taylor & Francis Group

Oxidative cleaning of reverse osmosis membranes during reclamation of steel wastewater

Haigang Li[1], Ping Yu*, Yunbai Luo

College of Chemistry and Molecular Sciences, Wuhan University, Wuhan 430072, P.R. China, Tel./Fax: +86 27 68752511; emails: hgli@ipe.ac.cn (H. Li), yuping@whu.edu.cn (P. Yu), ybai@whu.edu.cn (Y. Luo)

Received 8 April 2014; Accepted 28 December 2014

ABSTRACT

Oxidants in alkaline solutions were developed to regenerate reverse osmosis membranes that had been severely fouled during the reclamation of wastewater from steel production. The cleaning efficiency and kinetics of the processes were evaluated in parallel with the fouling formation. Analysis of primary foulant constituents using scanning electron microscope (SEM)-electron-dispersive X-ray microanalysis spectrometry and Fourier transform infrared spectroscopy (FTIR) suggested that organic fouling might be dominant. Analysis of wastewater constituents using gas chromatography–mass spectrometry indicated that aliphatic acids and long chain alkanes were likely to be the predominant foulants. The cleaning efficiency increased initially, and then decreased with increasing concentrations of the oxidant. Micro-analyzed by FTIR, SEM, and atomic force microscope, the membrane integrity was not destroyed by the oxidant under the proper cleaning conditions. Surface reaction kinetic expression based on fouling resistance decline was developed to delineate the process.

Keywords: Oxidant; Wastewater; Cleaning; Surface reaction; Fouling

1. Introduction

As demand for water increases worldwide, the reclamation of wastewater is gaining in popularity. Recently, reverse osmosis (RO) has become the leading technology for this application due to membrane cost reduction, process development, and operational experience. However, fouling largely constricts membrane performance, particularly when irreversible. Although wastewater is treated in a pretreatment step, it is inevitable that trace organic compounds remain in the effluent. Residual organic matter causes membrane fouling in the subsequent RO filtration. Furthermore, metal cations contribute to fouling by enhancing the aggregation of organic molecules in solution [1] and/or by neutralizing the negative charge of the membrane surface [2]. In the case of constant permeate flux operation, membrane fouling leads to a steady increase in operating pressure, a rise of 10% necessitates interruption of operation for routine cleaning [3].

Chemical agents are used to remove foulants from the membrane surface. Alkaline solutions, acid solutions, metal chelating agents, surfactants, and NaCl

*Corresponding author.
[1]Current address: Key Laboratory of Green Process and Engineering, Institute of Process Engineering, Chinese Academy of Sciences

solutions are typically used, either in combination or sequentially. The cleaning mechanisms of these agents have been comprehensively reported previously [4–6]. Chemical selection is dependent on the nature of foulants deposited on the membrane. Generally, individual cleaning agents are found to be effective, but too specific. For instance, alkaline solutions play an effective role in flux recovery of organic and microbial-fouled membranes [7]; however, show limited cleaning efficiency for combinations of foulants classes. A higher cleaning efficiency can be obtained by strategically pairing chemical agents due to complementary cleaning mechanisms [8].

Oxidants are extremely successful for regeneration of membranes, with sodium hypochlorite and hydrogen peroxide the most commonly applied [7,9,10]. When an ultrafiltration (UF) membrane is cleaned by a NaClO solution, full flux recovery is obtained [11]. While polyvinylidene fluoride membranes can stand several years of oxidative cleaning [12], the chlorine sensitivity of polyamide materials limits their oxidative cleaning, but research into the latter continues. Under controlled conditions (i.e. active chlorine concentration, contact time), membrane permeation flux can be improved while maintaining a high membrane retention [13]. Chlorination reactions with polyamide membranes are dependent on the solution pH [14], and at high pH (pH > 10), NaClO effectively removes organic foulants with almost negligible oxidation effects to the membrane [15].

Kinetic models of cleaning have been reported in the literature, but the results appear to be inconsistent. A first-order reaction is perhaps most frequently used to describe the cleaning process based on permeate flux recovery [16], or membrane resistance decline [17]. Contrastingly, Bird and Bartlett [18] have demonstrated that cleaning is not a first-order reaction. Koyuncu et al. [19] proposed a kinetic expression similar to the Hom-Hass model which is used in modeling disinfection. Therefore, in this work, we investigated the oxidative cleaning of RO membranes applied in a steel plant. The oxidative cleaning behavior was described by a surface reaction model. The cleaning kinetic equation of cleaning was determined. The findings of this study provide an additional mechanism of the oxidative cleaning.

2. Materials and methods

2.1. Membranes and wastewater

A fouled RO membrane element (Hydranautics, CPA2-4040) in almost 1-year service in a steel plant in Wuhan, Hubei Province, China, was selected for this work. CPA2 was a type of aromatic polyamide thin composite membrane supported by a polysulfone layer. A phosphonate-based antiscalant was used in the RO operation. The raw wastewater had undergone a pretreatment process including coagulation, flocculation (with limewater and aluminum sulfate), dissolved-air flotation and filtration, pH correction, 5 μm cartridge filtration, and UF. Membranes were cleaned with a 2 wt.% citric acid solution (pH 4) at a feed pressure beyond 10%. However, foulants would still accumulate and remain on/in the membranes despite the implementation of periodic cleaning. The RO feed water was analyzed and the results are shown in Table 1. The cations and anions were analyzed by an ICS-900 ion chromatograph (Dionex, Sunnyvale, USA). The feed water was organic and brackish in nature owing to the excellent UF removal of suspended solids during the pretreatment. Since the most appropriate cleaning agent is related to the nature of the foulants developing on the membrane surface, the nature of the fouling layer was first ascertained by instrumental analyses.

2.2. Membrane cleaning

Membranes were cleaned in a laboratory-scale cross-flow filtration setup with an oxidant solution (NaClO and H_2O_2) at pH 12.0. The setup (Fig. 1) consists of a round membrane cell, a high-pressure pump, an electromagnetic mixer, a feed tank, and a temperature control system. The cleaning solution was held in a 3.0 L tank and a membrane was placed in the membrane cell. Cleaning was performed at ordinary pressure and a cross flow velocity of 30.1×10^{-2} m s^{-1}.

Table 1
Quality of the secondary effluent

Parameter	Feed water
pH	7.6 ± 0.5
Turbidity (NTU)	0.27 ± 0.12
Conductivity (μS cm^{-1})	874.3 ± 10.2
Hardness (mg $CaCO_3$ L^{-1})	212.3 ± 5.2
COD (mg L^{-1})	23.4 ± 3.2
Mineral oil (mg L^{-1})	0.7 ± 0.1
Bicarbonate, HCO_3^- (mg L^{-1})	95 ± 17
Carbonate, CO_3^{2-} (mg L^{-1})	<1
Ca^{2+} (mg L^{-1})	59.6 ± 8.7
Al^{3+} (mg L^{-1})	78.5 ± 9.2
Fe (mg L^{-1})	144.5 ± 12.4
Cl^- (mg L^{-1})	133.5 ± 14.6
NO_3^- (mg L^{-1})	47.6 ± 3.2
SO_4^{2-} (mg L^{-1})	140.3 ± 21.2
PO_4^{3-} (mg L^{-1})	73.2 ± 6.7

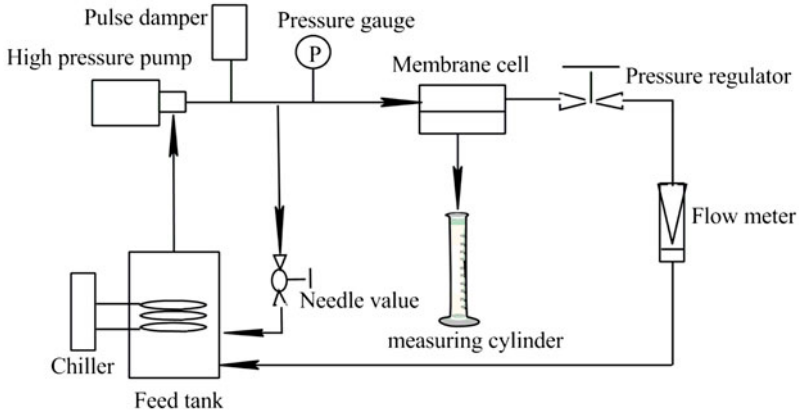

Fig. 1. Schematic of the laboratory-scale cross-flow RO filtration setup.

The solution was continuously circulated from the feed tank to the membrane for a period of 0.5, 1.0, 2.0, 3.0, 4.0, and 5.0 h separately. At the end of the cleaning, the membranes were rinsed with deionized (DI) water to flush out the chemical residue. Then, the pure water flux of a cleaned membrane was tested to determine the cleaning efficiency. The effects of operation parameters (including the concentration of oxidants, temperature, and time) on the cleaning efficiency were investigated. New membrane sheets cut from the membrane element were used for each cleaning mode.

2.3. Characterization methods

2.3.1. Fourier transform infrared spectroscopy

The attenuated total reflection-Fourier transform infrared spectroscopy (ATR-FTIR) was performed on a Nicolet AVATAR 360 FTIR Spectrophotometer. The spectra were recorded at 10 locations, and each spectrum was averaged from 64 scans. The foulants were stripped off by a sterile spatula and their FTIR spectra were also collected in the transmission mode to confirm the organic composition. Attention was paid not to cut the membranes. The membranes and the foulants were vacuum-dried at ambient temperature prior to FTIR spectroscopy analysis.

2.3.2. Scanning electron microscope-electron-dispersive X-ray microanalysis

The surface morphologies of the membranes and the elemental composition of the foulants were analyzed by a scanning electron microscope (SEM) equipped with an electron-dispersive X-ray microanalysis (EDX) spectrometer (both FEI Quanta 200, Holland). All membranes were vacuum-dried at ambient temperature and coated with a conductive sputtered gold layer before SEM analysis.

2.3.3. Atomic force microscope

Surface roughness was determined by an SPM-9500J3 atomic force microscope (AFM) (Shimadzu, Kyoto, Japan) in the contact mode. Silicon probes were coated by 30 nm thick aluminum. Membrane surface roughness was characterized by the root mean square, which is the deviation of the peaks and valleys from the mean plane [20].

2.3.4. Gas chromatography/mass spectrometry

The organic matter dissolved in the wastewater was characterized by gas chromatography/mass spectrometry (GC/MS). Samples for GC/MS analysis were prepared by micro-solid phase extraction using an HP-5MS capillary column (30 m length × 0.25 mm ID × 0.25 μm film thicknesses). Analysis was performed in a temperature-programmed mode with an initial temperature of 35℃ held for 8 min, followed by a ramp of 3℃ min^{-1} to 200℃. The ion source temperature was 250℃, and the carrier gas was high-purity helium gas. The spectra were searched in the library of National Institute of Standards and Technology. Together with the characteristics of the steel wastewater, we confirmed the components of the wastewater.

2.3.5. Contact angle

Contact angle was measured with a DSA100 automated contact angle goniometer (KRŰSS GmbH,

Hamburg, Germany). Each measurement was performed at least 12 times and the highest and lowest values were discarded before averaging.

2.3.6. Mechanical properties

Mechanical properties (tensile strength and strain at break point) of each wet membrane were measured using an AGS-J universal tensile meter (Shimadzu, Japan) under ambient conditions. Each measurement was performed at least 10 times at a stretching speed of 2 mm min^{-1}. The highest and lowest values were discarded before averaging.

2.3.7. Organic/inorganic ratio

The foulants were dried at 105°C until the weight loss was less than 0.2 mg. The dry weight was recorded as m_1. The dried foulants were iglossed at 550°C in an SX2-10-12 muffle furnace (Experimental Electric Furnace Plant, Shanghai, China). Iglossed sample was weighed and recorded as m_2. The organic/inorganic ratio (δ) can be quantified as follows:

$$\delta = \frac{m_1 - m_2}{m_2} \tag{1}$$

2.4. Calculations

DI water flux was tested at the start and the end of each mode of cleaning. The cleaning efficiency (η) was evaluated as follows:

$$\eta = \frac{J_{\text{cleaned}}}{J_{\text{fouled}}} \tag{2}$$

where J_{cleaned} is the flux through a cleaned membrane, and J_{fouled} is the flux through a fouled membrane. The flux after 20 min of filtration by the DI water was determined. The filtration conditions were set at follows: operation pressure at 10 bar, temperature at 25°C, and cross-flow velocity at 2.9×10^{-2} m s^{-1}.

The concentrations of inorganic and organic compounds in the permeate during the wastewater reclamation should also be controlled. The rejection of the cleaned membranes was tested using the steel wastewater. The permeate and the feed samples were both collected at the start (20 min after start) and the end (20 min before termination) of the test. The concentration of the organics was measured by a chemical oxygen demand (COD) analyzer (Camlab CW2020 Colorimeter, HACH, USA), while salt concentration was determined by a DDS-12DW conductivity meter (Shanghai Benson Instrument Co., Ltd., China). The rejection properties of the membranes can be estimated as follows:

$$\xi = \left(1 - \frac{C_p}{C_f}\right) \times 100 \tag{3}$$

where ξ is the rejection rate, C_p and C_f are concentrations in the permeate and the feed, respectively.

The membrane resistance offered by the fouling deposit could be calculated from Darcy's law. The resistances attributed to the membrane and the fouling layer were assumed to act in series, and thus, the membrane permeate flux could be estimated as follows [21]:

$$J = \frac{\Delta P}{\mu R_{\text{TOT}}} = \frac{P - \sigma\Delta\pi}{\mu(R_m + R_F)} \tag{4}$$

$$R_F = \frac{\Delta P}{\mu J} - R_m \tag{5}$$

where P is the operation pressure, $\Delta\pi$ is osmotic pressure of solution, μ is the water viscosity, σ is the degree of permselectivity, R_{TOT} is the total membrane resistance, R_m is the intrinsic membrane resistance, R_F is the fouling resistance, and $\Delta P = P - \sigma\Delta\pi$ is the transmembrane pressure.

3. Results and discussion

3.1. Foulant characteristics

The SEM image in Fig. 2 clearly shows the formation of a fouling layer on the membrane surface. This is the dominant fouling mechanism for RO membranes because they are considered as dense membranes [22]. Surface fouling leads to a flux decline due to an increasing hydraulic resistance to permeate flow.

EDX of foulants (Fig. 3) shows carbon and oxygen as the two dominant elements. However, small quantities of metal such as Si, Al, and Fe are also found. These multivalent metallic elements are probably inorganic colloids entrapped in the organic fouling layer or complexed with accumulated organic molecules. These results indicate that the organics are the primary constituent of foulants. Validating this, the organic/inorganic ratio was calculated as 3.25 coinciding with the conclusion obtained by the SEM–EDX analyses (Fig. 3).

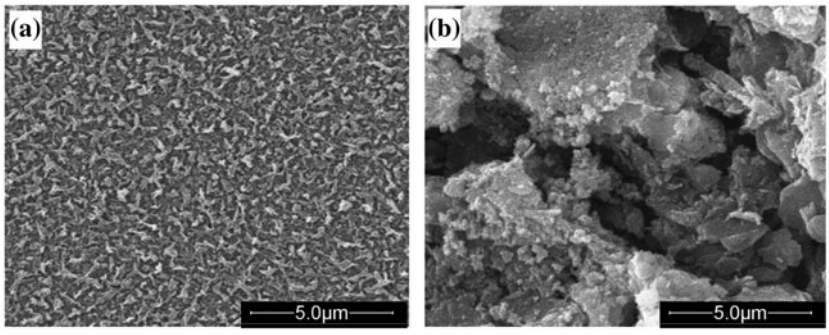

Fig. 2. Morphology of (a) virgin membrane and (b) fouled membrane.

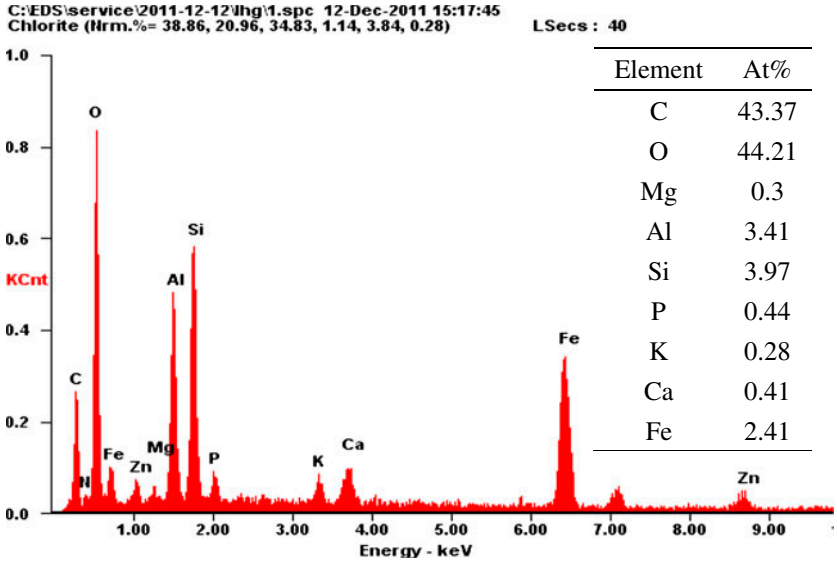

Element	At%
C	43.37
O	44.21
Mg	0.3
Al	3.41
Si	3.97
P	0.44
K	0.28
Ca	0.41
Fe	2.41

Fig. 3. EDX of physically stripped foulant layer.

The FTIR spectrum of foulants (Fig. 4) shows distinct peaks at 3,300 (hydroxyls), 2,917 (aliphatic chains), 1,645 (dissociated carboxylic group), 1,415 (aliphatic chains), and 1,028 cm^{-1} (hydroxyls). The spectrum indicates that the foulant contains typical aliphatic chains of fatty acid and long chain alkane [23]. The most abundant organics, as shown in Fig. 5, were long chain alkanes (4.2–17.2 min), n-hexadecane acid (18.3 min) and dibutyl phthalate (19.1 min). From a combination of the FTIR and GC/MS results, we conclude that the organics accumulated on the membrane surface were likely to be N-hexadecane acid and long chain alkanes.

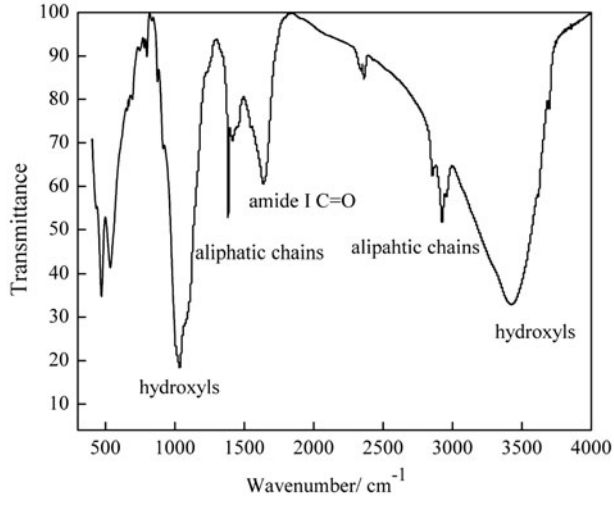

Fig. 4. FTIR spectrum of physically stripped fouling layer.

3.2. Oxidative cleaning of membranes

The organics had been proved as the primary constituents of the foulants. NaClO and H_2O_2 are the

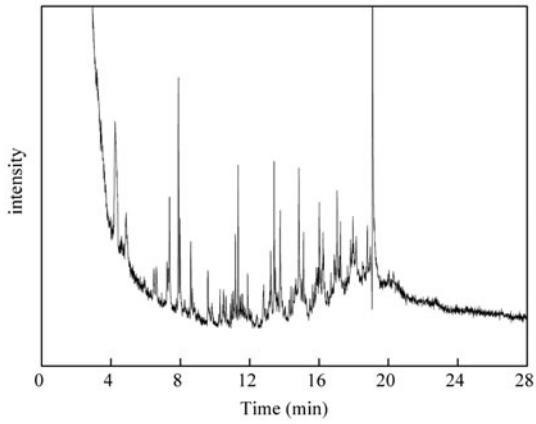

Fig. 5. The total GC chromatogram of the dissolved organic matter.

oxidants commonly used to remove organic foulants from membrane surface. Therefore, NaClO and H_2O_2 in alkaline environment (pH 12.0) were used to restore the membrane flux. As shown in Fig. 6, the flux increased with the cleaning time and stabilized after 4.0 h. The oxidants degraded the organic foulants to small molecules containing carboxyl, ketonic, and aldehyde groups, which made the foulants more susceptible to hydrolysis at high pH [7,24]. On the other hand, the aqueous alkali promoted the formation of a looser fouling layer that propelled the oxidant to enter the fouling layer. When membranes are cleaned near pK_a (pH 11.5), however, H_2O_2 will decompose to several active species including the perhydroxyl anion (OOH^-), hydroxyl radical (•OH), and superoxide anion radical ($•O_2^-$) [25]. In this case, the oxidation occurs more easily. However, after some time, further cleaning did not significantly remove the persistent foulants from the membrane surface.

It is notable that the concentration of the oxidant significantly affects the cleaning efficiency. The cleaning rate was quickened by the increase of oxidant concentration. With H_2O_2 concentration improved from 10 to 40 mM, the normalized flux of the cleaned membrane increased from 1.57 to 1.88 (Fig. 6(a)). With NaClO concentration rising from 1.34 to 5.37 mM, the normalized flux increased from 1.54 to 2.08 (Fig. 6(b)). However, overdose can unintendedly and detrimentally reduce the membrane performance. The changes of the water flux with oxidant concentration may be explained by the mass transfer, in which the molecules of the oxidant agent moved from the bulk solution to the fouling layer. When the fouled membrane is cleaned with an oxidant aqueous solution, the oxidant molecules will diffuse into the fouling layer.

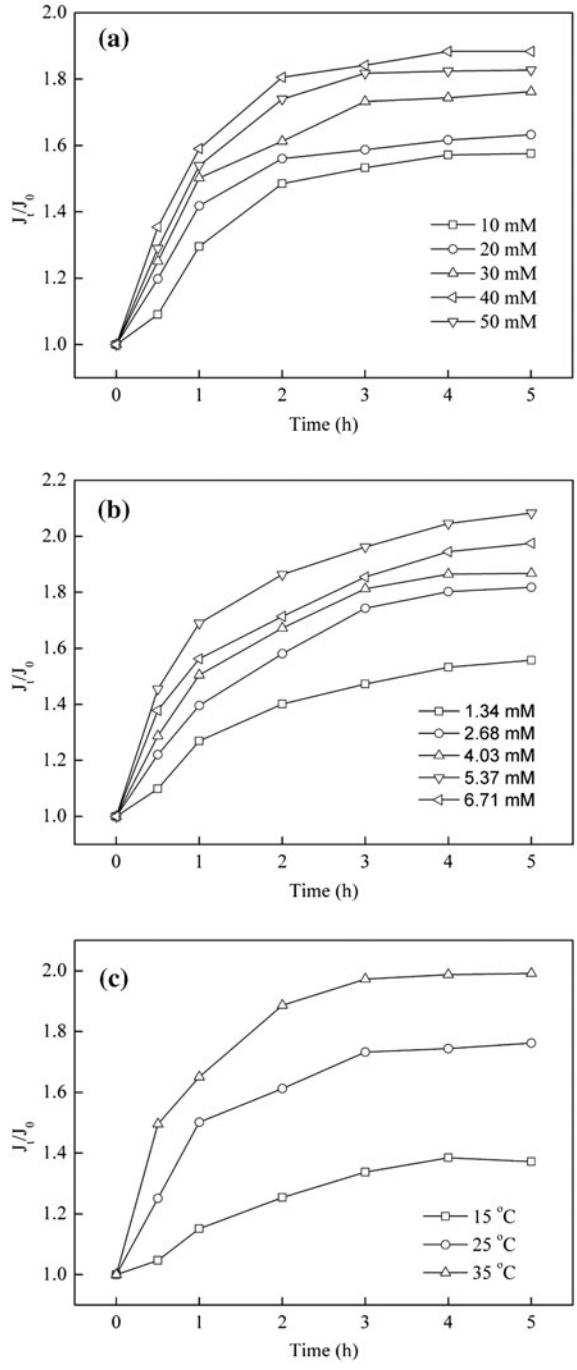

Fig. 6. DI water flux recovery at different cleaning conditions: (a) different H_2O_2 concentrations at temperature 25℃, (b) different NaClO concentrations at temperature 25℃, (c) various solution temperatures at H_2O_2 concentration 40 mM, and (d) various solution temperatures at NaClO concentration 5.37 mM.

Thus, at higher dosages, the amount of oxidant molecules diffusing into the fouling layer will be improved. With further increase in the concentration, however,

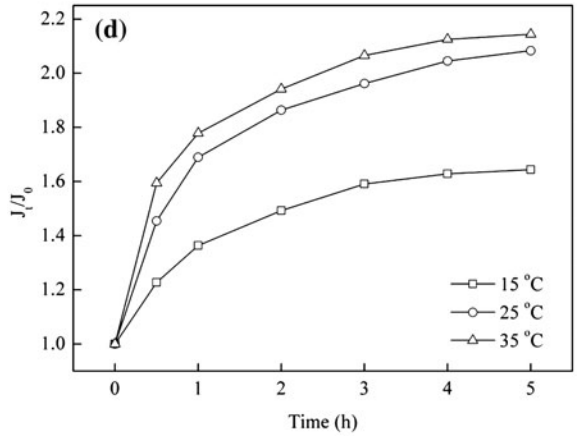

Fig. 6. (*Continued*)

the cleaning efficiency is reduced. Excessive amount of the oxidant will chemically degrade the membrane materials, resulting in flux reduction. As reported, the decline in water flux after membrane chlorination is attributed to membrane tightening [26] and/or the conformation of a more rigid polymer [27]. In contrast, the flux increases as a result of the cleavage of polyamide chains [28]. In our study, the flux decreased, which is contributed to membrane chlorination caused by the excess of oxidant molecules.

As shown in the flux curves at different cleaning temperatures (Fig. 6(c) and (d)), the flux restored faster at higher temperature. However, the effect is insignificant at high temperature, especially in the case of NaClO cleaning. Raising the temperature could accelerate the cleaning process [29]. A higher cleaning temperature leads to a faster adsorption of the oxidant, because the increasing kinetic energy of the molecules promotes the adsorption of the oxidant molecules onto the foulant layer. Therefore, the relatively high temperature will favorably activate the oxidation. In addition, the high temperature promotes the transport of reaction products from the fouling layer into the bulk solution. However, the effect of the increasing temperature is limited by the thermal sensitivity of the membrane materials.

The cleaning cost was estimated simply (Table 2). The cost calculation only included the cost of oxidants, but excluded the costs of electricity, water, disposal, labor, or other miscellaneous items, because our aim was to estimate conceptual cost. The cost of the NaClO cleaning mode is lower than that of the H_2O_2 cleaning mode at varying temperatures. These results indicate the higher efficiency and lower cost of NaClO than H_2O_2.

3.3. Characterization of the cleaned membranes

3.3.1. Membrane performance

Fig. 7(a) shows notable flux decline vs. filtering time after membrane cleaning. In contrast, the flux through the fouled membranes was stable, probably it approached the pseudo-stable level. The oxidant can oxidize and remove the organic foulants very effectively, especially in the NaClO solution. The cleaned membranes were reused in the reclamation of the steel wastewater. The readhesion of the foulant onto the membrane surface led to a discernible flux decline. However, the cleaned membrane generated a significantly greater flux than the fouled membrane did.

The rejection test was also carried out. The separation properties of the membranes were improved after the oxidative cleaning (Fig. 7(b) and (c)). The salt rejection was improved slightly, while the COD rejection increased more discernibly. The increase is attributed to the increased hydrophilicity of the membrane surface. The hydrophilic surface inhibits the foulants from readsorption onto the membrane surface. The enhanced rejection can be also attributed to the increasing water flux, which results in lower COD and salt concentrations in the permeate. The change in

Table 2
Cost estimation of the cleaning

Cleaning mode	Unit price of chemicals ($ t^{-1})	Amount of agents (mM)	Flux recovery (μm s^{-1})			Cost per flux recovery × 10^4 ($ s μm^{-1})		
			15℃	25℃	35℃	15℃	25℃	35℃
NaClO	122–163[b]	10.74	8.30	13.80	14.85	1.17–1.58	0.70–0.95	0.65–0.88
H_2O_2	163–187[c]	80.00	5.07	9.82	12.03	3.18–3.64	1.64–1.88	1.34–1.53

[a]Data from China Chemical Network (http://www.chinachemnet.com/).
[b]The price of 10.0 wt.% NaClO solution.
[c]The price of 27.5 wt.% H_2O_2 solution.
[d]The volume of cleaning solution is 2.0 L.

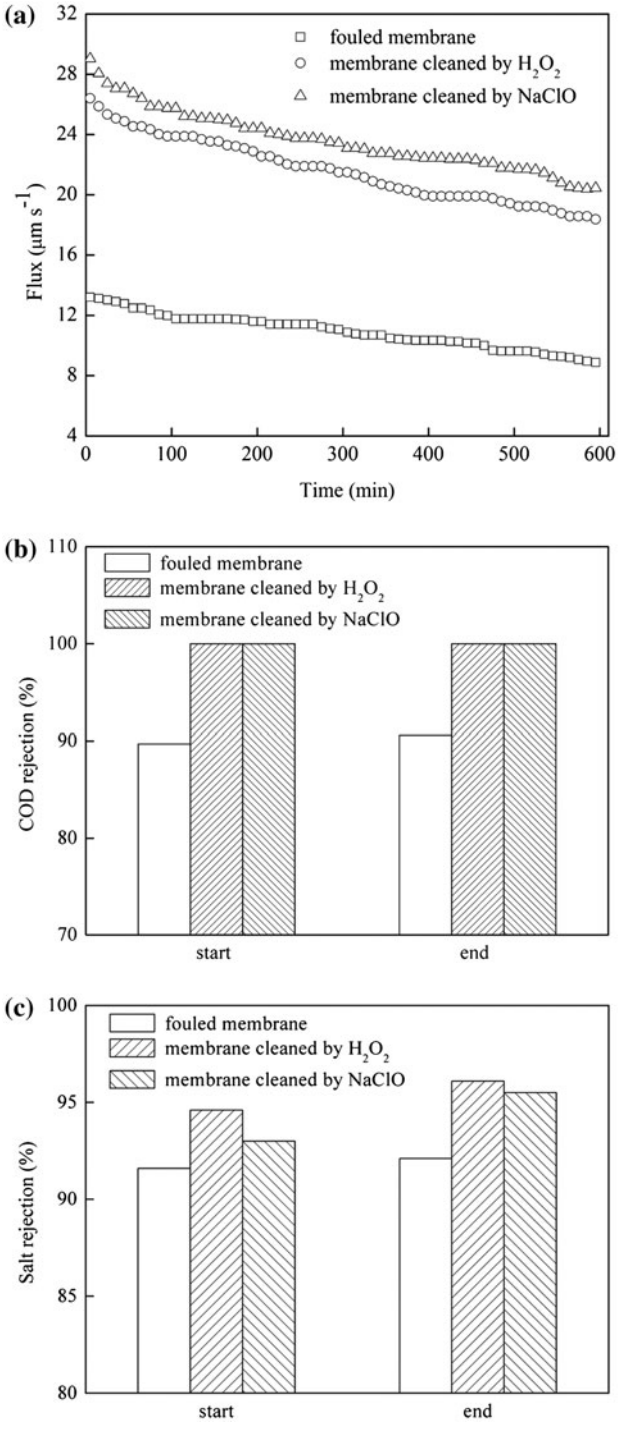

Fig. 7. Membrane performance after oxidative cleaning: (a) flux stability; (b) COD rejection; (c) salt rejection. Cleaning condition: H_2O_2 concentration = 40 mM, NaClO concentration = 5.37 mM, cleaning temperature = 35°C, solution pH 12.0, and cleaning time = 4.0 h.

contact angle on the membrane surface is a good indicator of the cleaning efficiency [30]. The surface contact angles dramatically dropped from 63.5° (fouled membrane) to 29.2° (H_2O_2-cleaned membrane) and 24.2° (NaClO-cleaned membrane). The surface contact angles of the cleaned membranes were close to that of the virgin membrane (22.4°).

Table 3
Mechanical properties of membranes

Membrane	Tensile strength (MPa)	Strain at break (%)
Virgin	79.5 ± 3.3	18.9 ± 1.2
Fouled	73.6 ± 3.5	18.7 ± 0.6
Cleaned by H_2O_2	71.3 ± 2.3	17.7 ± 0.9
Cleaned by NaClO	70.8 ± 1.5	17.0 ± 1.1

The mechanical properties were also tested and the results are listed in Table 3. The mechanical properties of the membranes deteriorated after 1-year of service in the steel plant. The tensile strength was more sensitive than the strain at break point. However, the mechanical properties of the cleaned membranes were similar to those of the fouled membrane, indicating that the effect of oxidation on membranes is almost negligible at high pH.

3.3.2. Membrane surface characterization

As shown in Fig. 8, the virgin membrane showed the main characteristic bands at 1,243, 1,295, and 1,327 cm^{-1} (stretching of aromatic amines I, II and III), 1,490 and 1,585 cm^{-1} (polysulfonyl group), 1,545 (amide I), and 1,665 cm^{-1} (amide II) [31–33]. After the formation of a thin foulants layer on the membrane surface, the absorbance spectra of the underlying

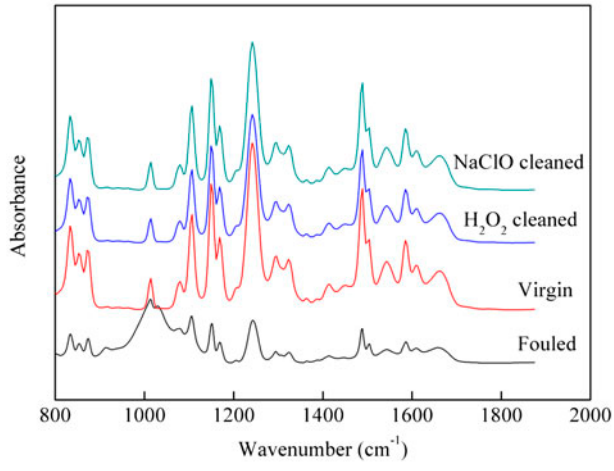

Fig. 8. ATR-FTIR spectra of membranes.

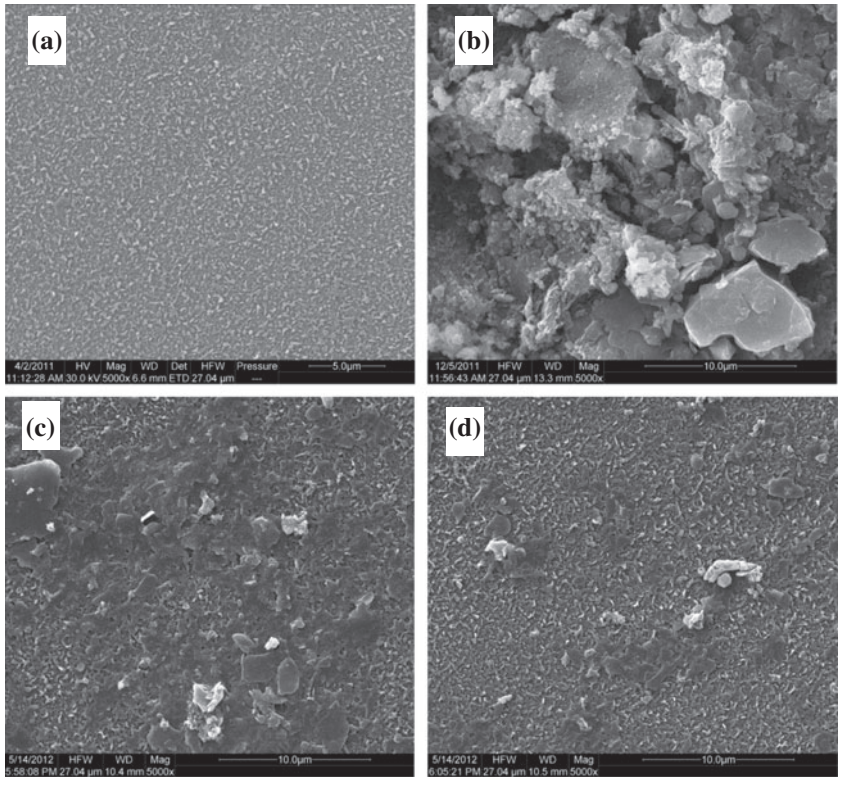

Fig. 9. SEM images of membranes with 5,000 times magnification: (a) virgin membrane, (b) fouled membrane, (c) membrane cleaned by H_2O_2, and (d) membrane cleaned by NaClO.

polyamide composite membranes became less apparent, and the characteristic peaks of aromatic amines disappeared. Meanwhile, the absorbance intensity of the peak at about 1,030 cm^{-1} (hydroxyls) was improved. The spectral profiles of after oxidative cleaning and the virgin membranes were similar. The peaks of the foulants disappeared and the characteristic peaks of the polyamide membranes reappeared. It was noted that the characteristic peaks were enhanced more significantly when a higher cleaning efficiency was achieved using NaClO (pH 12.0).

The SEM images (Fig. 9) show the changes of membrane surface morphology. The image of the virgin membrane shows a pebble-style surface with peaks and valleys. In comparison, the fouled membranes are obviously covered by the foulants which initially deposit and accumulate on the membrane surface. Then the foulants cover the membrane surface over time to form a fouling layer. The cleaned membranes become similar to the virgin membrane in terms of surface morphology. After cleaning by H_2O_2 solution, the pebble-style surface reappeared. After cleaning with NaClO solution, the pebble-style surface was more apparent and the area covered by foulants was constricted. These results indicate that the removal of foulants from the membrane surface is facilitated by the use of the NaClO solution.

The AFM images of the membrane surface (Fig. 10) indicate that the changes on the fouling surface are largely consistent with the SEM images (Fig. 9). In our previous study [4], the surface roughness of the virgin membrane was estimated to be 111.8 nm. The largest surface roughness was found in the fouled membrane (346.2 nm), because the surface roughness increased with the presence of the foulants. After cleaning by the H_2O_2 solution, the surface roughness of the fouled membrane decreased to 169.7 nm due to the removal of foulants. After cleaning by NaClO solution, the surface roughness decreased more strikingly (133.4 nm). The surface roughness was extremely close to that of the virgin membrane, indicating that almost all foulants were removed off from the polymer surface.

3.4. Cleaning kinetics modeling

With the oxidative cleaning, the oxidation occurred on the fouling layer but not in the cleaning solution. In this work, we propose a single-site surface reaction model based on the decline of fouling resistance. The

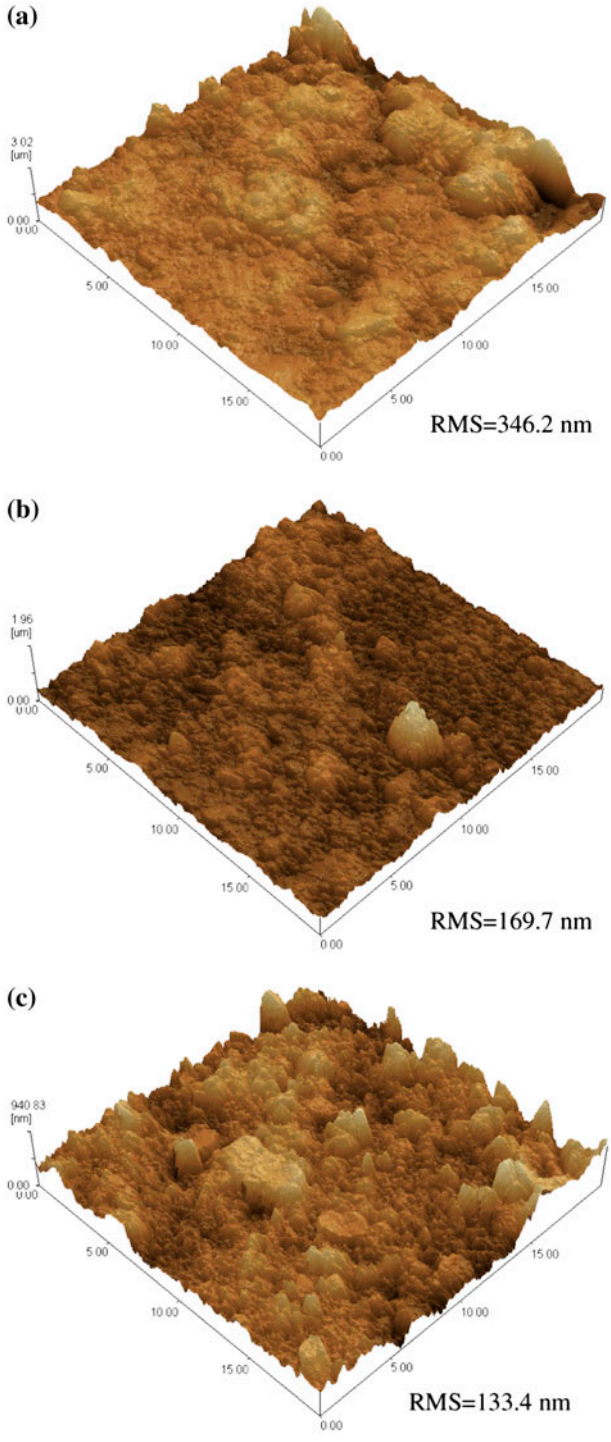

Fig. 10. AFM image of (a) fouled membrane, (b) membrane cleaned by H_2O_2, (c) membrane cleaned by NaClO. Each side of plane is 20 μm.

surface reaction is an additional mechanism of membrane cleaning. The oxidative cleaning process can be viewed as a three-step sequence. First, the oxidant is adsorbed onto the fouling layer. Second, the foulants and oxidants react on the fouling layer. As a result, the bonds between the foulants and the membrane surface break down and/or the foulants decompose to small molecules. Finally, the oxidation products transport to the bulk solution and then are sheared away. This situation is similar to the research on the

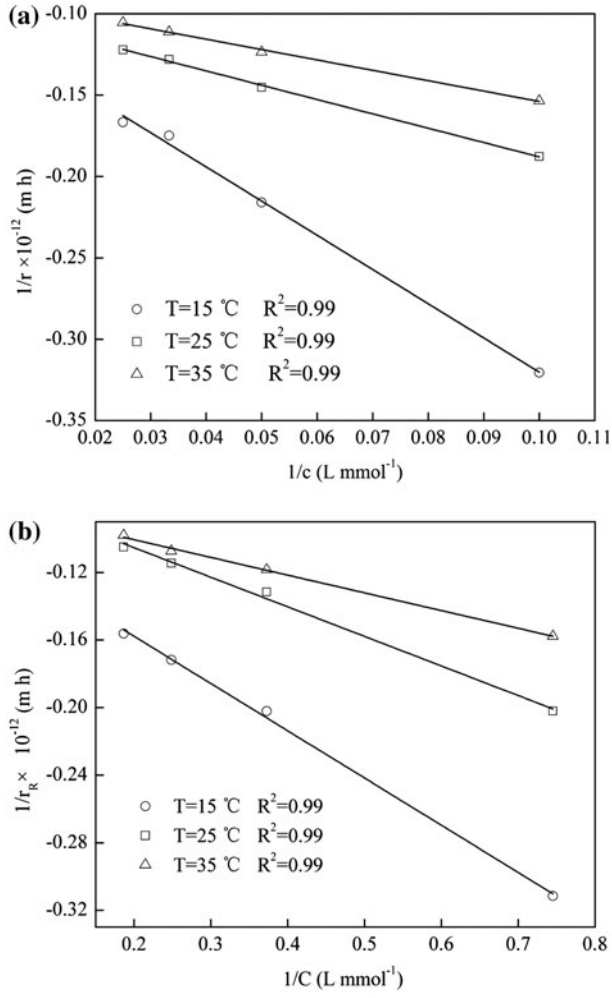

Fig. 11. Reciprocal the initial cleaning rate vs. reciprocal oxidant concentration: (a) H_2O_2, (b) NaClO.

Table 4
Temperature dependence of k_c and K_O in oxidative cleaning processes

	Temperature (℃)		
	15	25	35
k_c (m^{-1} s^{-1}) H_2O_2 cleaning ($\times10^{-9}$)	2.53	2.78	3.06
k_c (m^{-1} s^{-1}) NaClO cleaning ($\times10^{-9}$)	2.73	3.35	3.97
K_O (L mol^{-1}) H_2O_2 cleaning	52	110	140
K_O (L mol^{-1}) NaClO cleaning	0.064	0.080	0.083

adsorption and oxidation of the organics using the membrane [34]. The surface reaction rate law is expressed as follows [35]:

$$r = k\theta_F\theta_O \quad (6)$$

where r is the oxidative reaction rate; k is reaction rate constant; θ_F and θ_O are membrane surface coverage by the foulants and the oxidants, respectively.

Surface reaction is assumed to be rate-controlling, and the surface coverage is computed by Langmuir model as follow:

$$\theta = \frac{KC}{1 + KC} \quad (7)$$

where K is the adsorption coefficient, and C is the concentration.

Before cleaning, the foulants were already adsorbed onto the membrane surface, and thus θ_F was 1.0. The oxidants were adsorbed onto the surface of the foulants during the cleaning. We assume that the decreasing rate of fouling resistance is equal to the oxidants-foulant reaction rate. Therefore, the cleaning rate law can be expressed as follows:

$$r_R = r = k_c\theta_O = k_c\frac{K_O C_O}{1 + K_O C_O} \quad (8)$$

where r_R is the initial declining rate of membrane resistance, k_c is the oxidative cleaning rate constant, K_O is the adsorption coefficient of the oxidants onto the foulants, and C_O is the concentration of the oxidant.

Then Eq. (8) can be rearranged as follows:

$$\frac{1}{r_R} = \frac{1}{k_c K_O}\frac{1}{C_O} + \frac{1}{k_c} \quad (9)$$

Eq. (9) is expressed in a straight line mode, which greatly facilitates the determination of the parameter.

The reduction of the fouling resistance follows the decay of surface reaction kinetics before the concentration of the cleaning solution is maximized. Laboratory-obtained flux data were transformed via Eq. (9). The curve decreased in a straight line with a related coefficient extremely near 1.0 (Fig. 11), which demonstrates that the oxidative cleaning process corresponds quantitatively to the surface reaction kinetics model. k_c and K_O are temperature-dependent as shown in Table 4. Moreover, the NaClO cleaning method shows a larger k_c and a higher cleaning efficiency than H_2O_2 cleaning method. These benefits can be contributed to the membrane swelling with the presence of chlorine, which generally promotes the transition of the cleaning agent to the foulant.

4. Conclusions

Organic fouling was found to be dominant during the reclamation of steel wastewater. The primary organic compounds were likely to be aliphatic acids and long chain alkanes. H_2O_2 and NaClO alkaline solution (pH 12.0) exhibited the great cleaning efficiency and obviously improved the performance of cleaned membranes, including permeate flux and rejection. In addition, under the optimal cleaning conditions, the organics deposited on the membrane surface were removed with almost negligible oxidation effects to the membrane. This oxidative cleaning was feasible for the regeneration of RO membranes in service for long times. Oxidative cleaning of the fouled membrane followed a surface reaction kinetics model. NaClO cleaning had the greater power than the H_2O_2 cleaning process.

Acknowledgement

This work was supported by the National Science and Technology Support Program [grant number 2012BAC02B03].

Nomenclature

J	—	permeation flux (μm s^{-1})
m	—	foulant weight (g)
C	—	concentration (mg L^{-1})
t	—	permeation measuring time (min)
r	—	oxidative reaction rate (mol h^{-1})
k	—	reaction rate constant (mol h^{-1})
r_R	—	the initial rate of membrane resistance decline (m^{-1} h^{-1})
k_c	—	cleaning rate constant (m^{-1} h^{-1})
K	—	Langmuir adsorption coefficient (L mol^{-1})
T	—	temperature (K)
P	—	operation pressure (bar)
R	—	resistance (m^{-1})

Greek letters

δ	—	organic/inorganic ratio
ξ	—	rejection rate

η	—	cleaning efficiency
θ	—	available site on the membrane surface
μ	—	viscosity (N s m^{-2})
$\Delta\pi$	—	osmotic pressure (bar)
σ	—	degree of permselectivity

Subscript/ superscript

p	—	permeate
F	—	the foulants
m	—	membrane
f	—	feed solution
O	—	oxidant

References

[1] W.Y. Ahn, A.G. Kalinichev, M.M. Clark, Effects of background cations on the fouling of polyethersulfone membranes by natural organic matter: Experimental and molecular modeling study, J. Membr. Sci. 309 (2008) 128–140.

[2] G. Amy, J. Cho, Interactions between natural organic matter (NOM) and membranes: Rejection and fouling, Water Sci. Technol. 40 (1999) 131–139.

[3] A. Al-Amoudi, R.W. Lovitt, Fouling strategies and the cleaning system of NF membranes and factors affecting cleaning efficiency, J. Membr. Sci. 303 (2007) 4–28.

[4] H. Li, Y. Lin, Y. Luo, P. Yu, L. Hou, Relating organic fouling of reverse osmosis membranes to adsorption during the reclamation of secondary effluents containing methylene blue and rhodamine B, J. Hazard. Mater. 192 (2011) 490–499.

[5] A. Simon, W.E. Price, L.D. Nghiem, Changes in surface properties and separation efficiency of a nanofiltration membrane after repeated fouling and chemical cleaning cycles, Sep. Purif. Technol. 113 (2013) 42–50.

[6] A. AL-Amoudi, Effect of chemical cleaning agents on virgin nanofiltration membrane as characterized by positron annihilation spectroscopy, Sep. Purif. Technol. 110 (2013) 51–56.

[7] N. Porcelli, S. Judd, Chemical cleaning of potable water membranes: A review, Sep. Purif. Technol. 71 (2010) 137–143.

[8] W.S. Ang, N.Y. Yip, A. Tiraferri, M. Elimelech, Chemical cleaning of RO membranes fouled by wastewater effluent: Achieving higher efficiency with dual-step cleaning, J. Membr. Sci. 382 (2011) 100–106.

[9] V. Puspitasari, A. Granville, P. Le-Clech, V. Chen, Cleaning and ageing effect of sodium hypochlorite on polyvinylidene fluoride (PVDF) membrane, Sep. Purif. Technol. 72 (2010) 301–308.

[10] I. Levitsky, A. Duek, E. Arkhangelsky, D. Pinchev, T. Kadoshian, H. Shetrit, R. Naim, V. Gitis, Understanding the oxidative cleaning of UF membranes, J. Membr. Sci. 377 (2011) 206–213.

[11] E. Zondervan, B. Roffel, Evaluation of different cleaning agents used for cleaning ultra filtration membranes fouled by surface water, J. Membr. Sci. 304 (2007) 40–49.

[12] P. Wang, Z. Wang, Z. Wu, Q. Zhou, D. Yang, Effect of hypochlorite cleaning on the physiochemical characteristics of polyvinylidene fluoride membranes, Chem. Eng. J. 162 (2010) 1050–1056.

[13] A. Ettori, E. Gaudichet-Maurin, J.C. Schrotter, P. Aimar, C. Causserand, Permeability and chemical analysis of aromatic polyamide based membranes exposed to sodium hypochlorite, J. Membr. Sci. 375 (2011) 220–230.

[14] C.J. Gabelich, J.C. Frankin, F.W. Gerringer, K.P. Ishida, I.H. Suffet, Enhanced oxidation of polyamide membranes using monochloramine and ferrous iron, J. Membr. Sci. 258 (2005) 64–70.

[15] A. Farooque, A. Al-Amoudi, A. Hassan, Chemical cleaning experiments for performance restoration of NF membranes operated on seawater feed, IDA Conference, 2002, Bahrain.

[16] X. Li, J. Li, X. Fu, R. Wickramasinghe, J. Chen, Chemical cleaning of PS ultrafilters fouled by the fermentation broth of glutamic acid, Sep. Purif. Technol. 42 (2005) 181–187.

[17] Q. Gan, J.A. Howell, R.W. Field, R. England, M.R. Bird, M.T. McKechinie, Synergetic cleaning procedure for a ceramic membrane fouled by beer microfiltration, J. Membr. Sci. 155 (1999) 277–289.

[18] M.R. Bird, M. Bartlett, CIP optimisation for the food industry: Relationships between detergent concentration, temperature and cleaning time, Trans. IChemE (Part) C 73 (1995) 63–70.

[19] I. Koyuncu, A. Lüttge, M.R. Wiesner, Interferometric observations and kinetic modeling of the chemical cleaning of humic materials deposited on membranes, J. Membr. Sci. 313 (2008) 127–134.

[20] E.M. Vrijenhoek, S. Hong, M. Elimelech, Influence of membrane surface properties on initial rate of colloidal fouling of reverse osmosis and nanofiltration membranes, J. Membr. Sci. 188 (2001) 115–128.

[21] K.J. Martin, D. Bolster, N. Derlon, E. Morgenroth, R. Nerenberg, Effect of fouling layer spatial distribution on permeate flux: A theoretical and experimental study, J. Membr. Sci. 471 (2014) 130–137.

[22] S. Lee, M. Elimelech, Relating organic fouling of reverse osmosis membranes to intermolecular adhesion forces, Environ. Sci. Technol. 40 (2006) 980–987.

[23] M.O. Maiko Okajima-Kaneko, K. Kabata, T. Kaneko, Extraction of novel sulfated polysaccharides from Aphanothece sacrum (Sur.) Okada, and its spectroscopic characterization, Pure. Appl. Chem. 79 (2007) 2039–2046.

[24] C.-F. Lin, S.-H. Liu, O.J. Hao, Effect of functional groups of humic substances on UF performance, Water Res. 35 (2001) 2395–2402.

[25] M. Li, C. Foster, S. Kelkar, Y. Pu, D. Holmes, A. Ragauskas, C. Saffron, D. Hodge, Structural characterization of alkaline hydrogen peroxide pretreated grasses exhibiting diverse lignin phenotypes, Biotechnol. Biofuels 5 (2012) 1–15.

[26] J. Glater, M.R. Zachariah, S.B. McCray, J.W. McCutchan, Reverse osmosis membrane sensitivity to ozone and halogen disinfectants, Desalination 48 (1983) 1–16.

[27] Y.-N. Kwon, J.O. Leckie, Hypochlorite degradation of crosslinked polyamide membranes, J. Membr. Sci. 283 (2006) 21–26.

[28] A. Simon, L.D. Nghiem, P. Le-Clech, S.J. Khan, J.E. Drewes, Effects of membrane degradation on the

removal of pharmaceutically active compounds (PhACs) by NF/RO filtration processes, J. Membr. Sci. 340 (2009) 16–25.
[29] J. Gu, H. Zhang, Z. Zhong, W. Xing, Conditions optimization and kinetics for the cleaning of ceramic membranes fouled by $BaSO_4$ crystals in brine purification using a DTPA complex solution, Ind. Eng. Chem. Res. 50 (2011) 11245–11251.
[30] M.R. Sohrabi, S.S. Madaeni, M. Khosravi, A.M. Ghaedi, Chemical cleaning of reverse osmosis and nanofiltration membranes fouled by licorice aqueous solutions, Desalination 267 (2011) 93–100.
[31] W. Lee, C.H. Ahn, S. Hong, S. Kim, S. Lee, Y. Baek, J. Yoon, Evaluation of surface properties of reverse osmosis membranes on the initial biofouling stages under no filtration condition, J. Membr. Sci. 351 (2010) 112–122.
[32] H. Li, Y. Lin, P. Yu, Y. Luo, L. Hou, FTIR study of fatty acid fouling of reverse osmosis membranes: Effects of pH, ionic strength, calcium, magnesium and temperature, Sep. Purif. Technol. 77 (2011) 171–178.
[33] H. Li, P. Yu, Y. Luo, Fouling mechanisms and primary foulant constituents in reverse osmosis membrane reclamation of a petrochemical secondary effluent, Desalin. Water Treat. (2014). doi:10.1080/19443994.2014.910138.
[34] L. Liu, G. Zheng, F. Yang, Adsorptive removal and oxidation of organic pollutants from water using a novel membrane, Chem. Eng. J. 156 (2010) 553–556.
[35] Z. Belohlav, P. Zamostny, A rate-controlling step in Langmuir–Hinshelwood kinetic models, Cana. J. Chem. Eng. 78 (2000) 513–521.